Performance evaluation and model-based optimization of the mainstream deammonification in an integrated fixed-film activated sludge reactor

Mohamad-Javad Mehrani [a,b], Mohammad Azari [c,*], Burkhard Teichgräber [d], Peter Jagemann [d], Jens Schoth [d], Martin Denecke [a], Jacek Mąkinia [b]

[a] Department of Urban Water- and Waste Management, University of Duisburg-Essen, Universitätsstraße 15, 45141, Essen, Germany
[b] Faculty of Civil and Environmental Engineering, Gdansk University of Technology, Ul. Narutowicza 11/12, 80-233, Gdansk, Poland
[c] Department of Aquatic Environmental Engineering, Institute for Water and River Basin Management, Karlsruhe Institute of Technology (KIT), Gotthard-Franz-Str. 3, Karlsruhe 76131, Germany
[d] EMSCHERGENOSSENSCHAFT and LIPPEVERBAND, Kronprinzenstrasse 24, 45128, Essen, Germany

HIGHLIGHTS

- Mainstream pilot-scale deammonification was simulated under seasonal temperature.
- Intermittent aeration strategy plays an important role in stable NOB suppression.
- The aeration was set to the optimized values (DO = 0.2 mgO$_2$/L, on/off ratio = 0.05).
- The nitrogen removal efficiency can enhance from 30% to > 50% (at optimized values).
- The nitrogen removal rate increased up to 25 gN/m^{3}d by optimized aeration values.

GRAPHICAL ABSTRACT
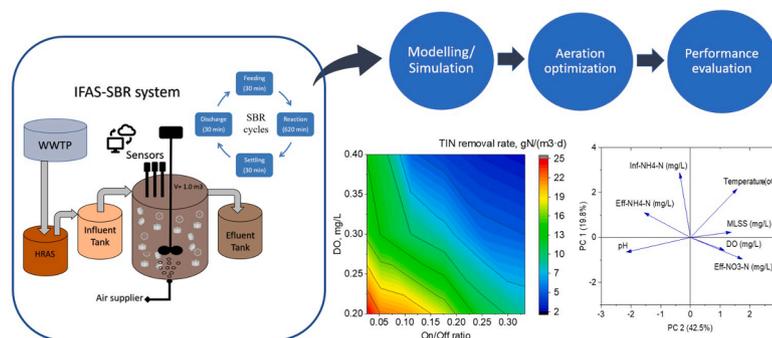
ARTICLE INFO

ABSTRACT

This study aimed to model and optimize mainstream deammonification in an integrated fixed-film activated sludge (IFAS) pilot plant under natural seasonal temperature variations. The effect of gradually decreasing temperature on the performance was evaluated during a winter season and a transition period to summer conditions, and the correlation of the performance parameters was investigated using principal component analysis (PCA). The optimization of intermittent aeration in the long-term (30 days) dynamic conditions with on/off ratio and dissolved oxygen (DO) set-point control was used to maximize the N-removal rate (NRR) and N-removal efficiency (NRE). Optimization results (DO set-point of 0.2–0.25 mgO$_2$/L, and on/off ratio of 0.05)

increased the NRE and NRR of total inorganic N (daily average) from 30% to > 50% and 15 gN/m^{3}d to 25 gN/m^{3}d, respectively. This novel long-term optimization strategy is a powerful tool for enhancing the efficiency in mainstream deammonification.

1. Introduction

Deammonification, also termed partial nitrification/anaerobic ammonium oxidation (anammox) or PN/A, is a sustainable and energy-efficient nitrogen removal process in wastewater treatment plants (WWTPs) (Gu et al., 2020). This process has widely been developed for sidestream treatment, such as anaerobic sludge digester liquors, but recently it has also been examined for treating wastewater in the mainstream (Izadi et al., 2021). However, the mainstream applications are facing numerous technical challenges, including stable PN and nitrite-oxidizing bacteria (NOB) suppression, sufficient anammox bacteria retention, a high carbon to nitrogen ratio (C/N), and influence of low temperature (Han et al., 2016; Gu et al., 2020).

The integrated fixed-film activated sludge (IFAS) process by combining flocs and biofilm can upgrade existing floccular activated sludge systems. The IFAS process produces less sludge, uses less energy, and brings a lower carbon footprint (Waqas et al., 2020). Moreover, IFAS is more robust than moving bed biofilm reactors (MBBRs) to achieve a more energy-efficient N-removal (Lemaire and Christensson, 2021; Malovanyy et al., 2015).

The key to efficient WWTP management is process optimization, which may be accomplished by searching for the best process conditions, such as aeration strategy, solid retention time (SRT), influent concentrations, and flow rates. Multi-objective optimization is a section of multiple criteria decision-making that assesses more than one objective function at the same time on a target (Newhart et al., 2019; Qiao & Zhang, 2018). NOB suppression is one of the most crucial challenges in deammonification systems (Mehrani et al., 2020; Gao & Xiang, 2021). An intermittent aeration strategy was reported as an effective solution for NOB diminishing (Miao et al., 2016; Van Hulle et al., 2010). Therefore, optimized intermittent aeration (switching between aerobic and anoxic phases) can enhance NOB suppression while reducing energy consumption and decreasing N$_2$O production (Al-Hazmi et al., 2021). Leix et al., (2017) optimized the deammonification process based on an aeration strategy, pH, and feeding parameters to enhance performance using a design of experiment (DOE) method. In other studies, the optimization of aeration parameters in IFAS was carried out using a combined experimental and computational fluid dynamic (CFD) approach (Xu et al., 2020; Zhou et al., 2019). In addition, based on model predictions, Al-Hazmi et al., (2021) optimized the aeration strategy (on/off cycles, frequency, and ratio) of a lab-scale granular deammonification sequencing batch reactor (SBR).

Nevertheless, there is still limited information for optimizing intermittent aeration and correlating related operational parameters in deammonification systems to suppress the NOB and to reach a higher nitrogen removal efficiency (NRE) and nitrogen removal rate (NRR) (Xu et al., 2020).

This study aims to model a stable long-term deammonification process for mainstream wastewater treatment (pilot-scale) to evaluate the following issues: i) estimation of the kinetic parameters for deammonification under dynamic temperature and C/N; ii) principal component analysis (PCA) to evaluate the correlation of the operational parameters on the system efficiency, and iii) model-based multi-objective optimization of the intermittent aeration strategy (DO concentration and on/off time) for maximizing the NRR and NRE. Additionally, most of the past studies on aeration strategy optimization were carried out in short-term operational conditions (batch tests or one cycle of a long-term experiment). On the contrary and as an initiative, this study investigates optimal aeration settings under the long-term (30 days) dynamic conditions.

2. Materials and methods

2.1. Experimental data for modeling purpose

2.1.1. Reactor setup

A one-stage pilot deammonification system (working volume of 1 m^3) was employed using an integrated fixed activated sludge (IFAS) process in a SBR. The reactor was installed at the WWTP Emscher-mündung near Dinslaken, Germany (EGLV) to treat real municipal wastewater. Biofilm carriers (AnoxKaldnes™ K3, Veolia) with a filling ratio of 20 % were used to provide conditions for anammox growth and accumulation. The reactor was previously seeded with anammox-rich sludge from a stably operating full-scale sidestream treatment reactor at Kamen-Körnebach WWTP near Dortmund, Germany (EGLV).

The reactor was initially operated with almost 12-hour batch cycles consisting of filling, reaction, sedimentation, and discharge phases. 120 L of wastewater were fed for 30 min into the reactor in the first phase, and the reaction phase lasted 620 min in total. To provide an intermittent aeration regime, the stage was divided into 20-minute on/off cycles. The aeration was on for 4 min and was off for 16 min as initial parameters, based on a former lab-scale study (Azari et al., 2020). During the aeration switched on phase, the DO concentration was initially set to 0.4 mg O$_2$/L (subject to the change as a control strategy parameter). To achieve a proper sludge settling and avoid biomass loss in the effluent, the sedimentation phase had been optimized at 30 min with no aeration or mixing. During the discharge phase (30 min), 120 L of the reactor content was discharged into the effluent container. Regular sampling (at least three times a week) was carried out in the influent tank, inside of the reactors, and in the effluent tank. The schematic layout of the SBR cycles can be found in supplementary materials (see supplementary material). To maintain a steady operation of deammonification, avoiding high organic loads and limiting the activity of heterotrophic denitrifiers (HET) are necessary (Hausherr et al., 2021). Hence, a carbon removal step, using a high-rate activated sludge (HRAS) reactor, was applied before the deammonification reactor, which can also capture the carbon for further energy recovery (Guven et al., 2019; Jimenez et al., 2015). The system also consisted of a 1 m^3 influent intermediate bulk container (IBC), into which the HRAS effluent was discharged and kept until it was pumped into the deammonification reactor.

Online sensors for DO, NO$_3$-N, NH$_4$-N, temperature, pH, and total suspended solids (TSS) (WTW, Xylem Analytics Germany Sales GmbH & Co) were installed on the top of the SBR, and the measurement outputs were sent to the central control unit via an SC1000 controller.

2.1.2. Analytical methods and calculations

Concentrations of ammonium (NH$_4$-N), nitrate (NO$_3$-N), nitrite (NO$_2$– N), total nitrogen (TN), and chemical oxygen demand (COD) were determined photometrically with DR3800 and corresponding cuvette tests (Hach-Lange, Germany). All samples were filtered through a 0.45 μm fiber filter before the analysis. The gravimetric technique was also used for total mixed liquor suspended solids measurement (MLSS) and its volatile fraction (MLVSS) to estimate the fraction of biomass in flocs and biofilm. MLSS concentration of flocs was also used for calibration of the TSS sensor for online monitoring (approximately in the range 3.0–4.0 g/L) during the experiment.

The calculated total inorganic nitrogen (TIN) comprised the sum of NH$_4$-N, NO$_2$– N, and NO$_3$-N. The process performance was assessed in terms of the NRE and NRR. The NRE was measured as the percentage of nitrogen removed in terms of both NH$_4$-N and TIN (Eq. (1)), and the NRR was determined for TIN (Eq. (2)).

1. Data collection:
➤ **Analytical data:** Nitrogen, biomass, and COD components
➤ **Sensor data:** pH, Temperature, DO, and flow rates

2. Model implementation
➤ The mantis2 model in GPS-X was selected for modeling of the nitrogen and COD removal process

3. Local sensitivity analysis
➤ Targets parameters are NH4-N, NO3-N, and COD
➤ Variables are operational and kinetic parameters

4. Dynamic calibration
➤ Experimental data at *winter season* (two months) was considered.
➤ For most important kinetics (Maximum growth rates) dynamic optimization was used.

5. Dynamic validation
➤ Experimental data at *summer season* (two months) was considered.
➤ Model efficiency performance (R^2, and RMSE) were applied

6. Performance analysis and optimization
➤ Correlation of process parameters using PCA
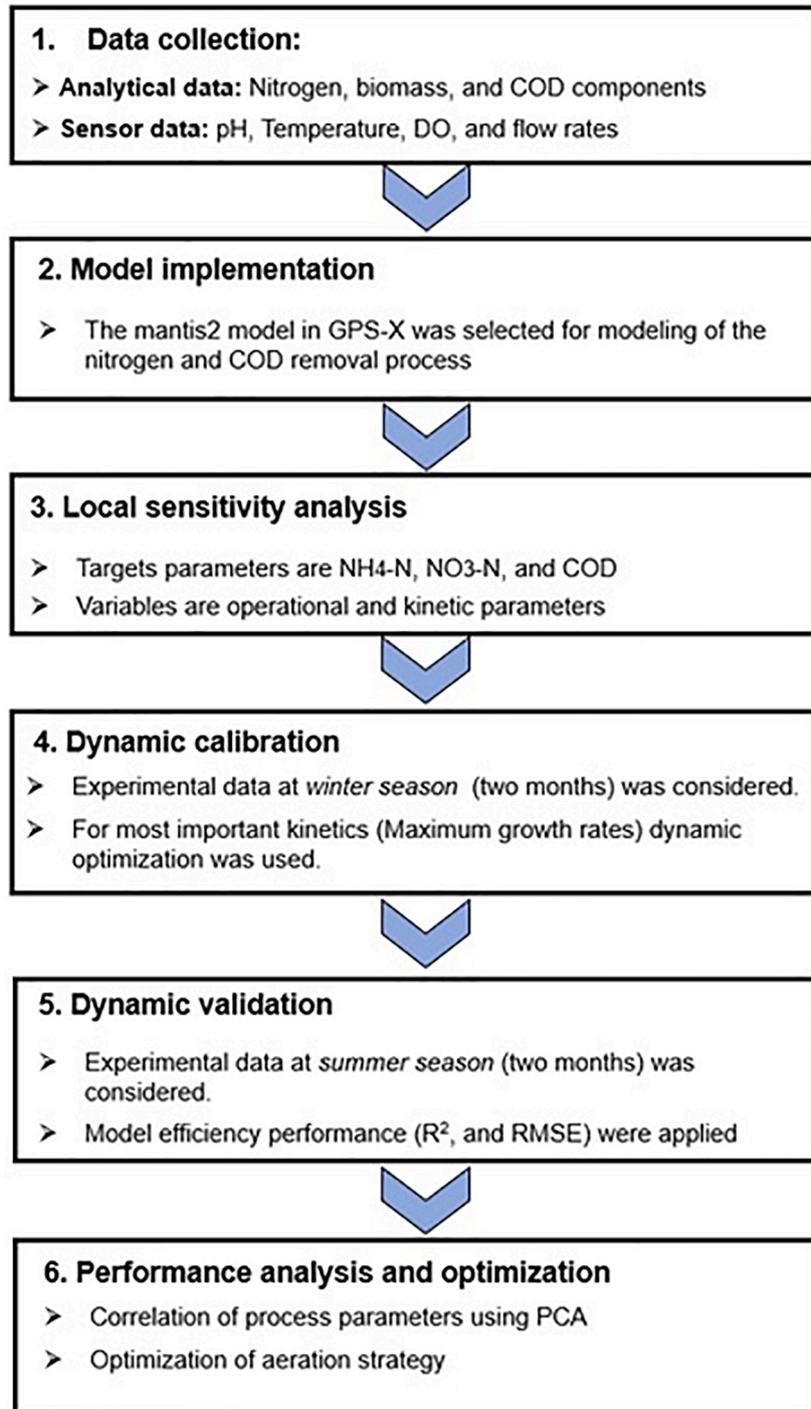➤ Optimization of aeration strategy

Fig. 1. Modelling, performance analysis, and optimization of the deammonification procedure.

$$NRE = \frac{N_i - N_e}{N_i} \times 100 \qquad (1)$$

$$NRR = \frac{Q \times (N_i - N_e)}{V} \qquad (2)$$

where N_i is nitrogen concentration in the influent (g/m^3), N_e is nitrogen concentration in the effluent (g/m^3), Q is a flow rate (L/d), and V is a volume of the system (L). The NRE and NRR are calculated as % and g N/m^{3}d, respectively.

2.2. Biokinetic model and simulation platform

The GPS-X (Hydromantis, Canada) is an open simulation and analysis platform for different wastewater treatment systems compatible with a sensitivity analysis (SA) (section 2.4.1) and optimization based on the Nelder-Mead simplex method (section 2.4.2) (Chang, 2012). The Mantis2 model, implemented in GPS-X 8.0, was used for modeling the studied pilot-scale deammonification system. The core model structure is based on the Activated Sludge Model No. 2d (ASM2d) (Henze et al., 1999) and Anaerobic Digestion Model No. 1 (ADM1) (Batstone et al., 2002). The model was extended to incorporate two-step nitrification and anammox processes (Abou-Elela et al., 2016; Sean et al., 2020). This

Table 1
Initial values of the kinetic parameters.

Bacteria	Kinetic parameter	Unit	Initial values
AOB	μ_{AOB}	1/d	1.01
	$K_{NH4,AOB}$	mg N/L	0.675
	$K_{O,AOB}$	mg O_2/L	0.30
	b_{AOB}	1/d	0.15
NOB	μ_{NOB}	1/d	0.31
	$K_{NO2,NOB}$	mg N/L	0.057
	$K_{O,NOB}$	mg O_2/L	0.2
	b_{NOB}	1/d	0.05
AMX	μ_{AMX}	1/d	0.03
	$K_{NH4,AMX}$	mg N/L	0.07
	$K_{NO2,AMX}$	mg N/L	0.05
	$K_{O,AMX}$	mg O_2/L	0.01
	b_{AMX}	1/d	0.003
HET	μ_{HET}	1/d	2.0
	$K_{NH4,HET}$	mg N/L	0.01
	$K_{NO3,HET}$	mg N/L	0.2
	$K_{NO2,HET}$	mg N/L	0.2
	$K_{O,HET}$	mg O_2/L	0.2
	b_{HET}	1/d	0.6

AOB: ammonia oxidation bacteria, NOB: nitrite oxidation bacteria, AMX: Anammox, HET: Heterotroph bacteria, K: half saturation coefficient, μ: maximum specific growth rate, b: specific decay rate,.

model has been used to simulate and optimize different wastewater treatment systems, especially deammonification systems (Pekyavas et al., 2020; Puchongkawarin et al., 2015; Sean et al., 2020). The IFAS-SBR reactor contains two different technologies of IFAS and SBR. However, GPS-X has IFAS and SBR reactors separately and cannot run them in a single system. Hence, this modeling study was carried out by applying an advanced SBR and assuming the apparent kinetics for the biochemical processes (Baeten et al., 2019).

2.3. Initial conditions

For dynamic calibration and validation of the models, the initial biomass concentrations for MLSS, MLVSS, and other microorganisms are needed (Yu et al., 2020). In this study, the microbiological tool was used to estimate the initial values of MLSS, MLVSS as well as ammonia-oxidizing bacteria (AOB), NOB, anammox bacteria (AMX), and HET initial population (relative abundance) using 16S rRNA gene high-throughput amplicon sequencing, based on previous assays (Azari et al., 2021). An example of 16S rRNA gene high-throughput amplicon sequencing results in the same period of the modelling study can be found in the supplementary material (see supplementary material). Also, Table 1 shows the initial kinetic parameters selected for sensitivity analysis and calibration procedure.

2.4. Simulation, validation, and optimization procedures

Calibration and validation are crucial steps in the modeling process that examine the model prediction capacity and reliability under various operating conditions. In this study, the mantis2 model (section 2.2) was first calibrated based on the data from a winter period (60 days) and then validated with another 60 days dataset from a summer period of the IFAS-SBR reactor. The calibration procedure was started with SA to find out the most sensitive parameters to optimize the kinetic parameters. Then, based on SA results, optimization of kinetic parameters based on experimental observation was done, and then, model performance with different performance criteria (R^2, RMSE, and MAE) was checked. Moreover, validation of the calibrated model with different periods of experimental observation were done to show the validity of the model. Fig. 1 shows the whole simulation/optimization procedure, and the most critical steps are discussed in the following subsections.

2.4.1. Sensitivity analysis

Sensitivity analysis is a method for determining the influence of one or more uncertain variables on some important results or quantities in mathematical models (Hong et al., 2019). In this study, 19 kinetic parameters targeting the N components (NH_3-N, NO_3-N) and COD concentrations were subjected to SA under the phase dynamic mode in GPS-X. Table 1 shows the initial values for the kinetic parameters under investigation. The uncertainty of 20% ($\pm10\%$ of the modified value) was assigned to each evaluated parameter (Lu et al., 2018). The ratio of the percentage change ($\Delta y_{i,j}/y_i$) in the *i-th* output variable (y_i) to the percentage change ($\Delta x_j/x_j$) in the *j-th* model parameter (x_j) was defined as the normalized sensitivity coefficient ($S_{i,j}$):.

$$S_{i,j} = \left| \frac{\Delta y_{i,j}}{y_i} \cdot \frac{x_j}{\Delta x_j} \right| \tag{3}$$

The following classification determines the impact of each modified parameter on the specific model result: i) low influential ($S_{i,j} < 0.25$), ii) influential ($0.25 \leq S_{i,j} < 1.0$), iii) high influential ($1.0 \leq S_{i,j} < 2.0$), and iv) extremely influential ($S_{i,j} \geq 2.0$).

2.4.2. Selection of the kinetic parameters based on optimization in GPS-X

Parameter Optimizer uses the Nelder-Mead simplex method with different objective functions to search for the parameter values with the minimum variance between measured data and model predictions (Chang, 2012). The optimization method was repeated until all sizes of the measured parameters decreased below the parameter tolerance (Lu et al., 2018).

Based on the SA results, high and extremely sensitive ($S_{i,j} \geq 1.0$) kinetic parameters were selected for estimation using the GPS-X optimization utility, and the least influential parameters ($S_{i,j} < 1.5$), were determined based on the literature in Table 1 (Mehrani et al., 2021; Yu et al., 2020; Al-Hazmi et al. 2021).

2.4.3. Comparison of model efficiencies

Various evaluation measures can be used to assess the model efficiency (goodness-of-fit), including the coefficient of determination (R^2), root mean square error (RMSE), and mean absolute error (MAE) which are frequently used. The RMSE measures the overall error in the same unit as the response variable, while the MAE assesses the quality of a predicted fluctuation and unbiasedness (Eq. 4–8). The R^2 measures the goodness-of-fit of a model based on experimental observations with a linear relationship. A model with accurate prediction has higher R^2 values (up to 1.0) (Hauduc et al., 2015).

$$SS_{tot} = \sum_i (y_i - \bar{y})^2$$

$$SS_{res} = \sum_i (y_i - f_i)^2$$

$$R^2 = 1 - \frac{SS_{res}}{SS_{tot}}$$

$$MAE = \frac{1}{n} \sum_i (y_i - f_i)$$

$$RMSE = \sqrt{\frac{SS_{res}}{n}} \tag{8}$$

where n is the total number of records, and i = 1, 2,..n is the number of observations. Also, SS_{res} is a residual sum of squares, and SS_{tot} is a total sum of squares of residuals, considering to y_i as a predicted value , f_i as an observed value, and $\bar{y}$ as an average value.

2.4.4. Aeration optimization strategy

Optimization of the aeration strategy to minimize TIN concentration was carried out by defining several scenarios for DO concentrations
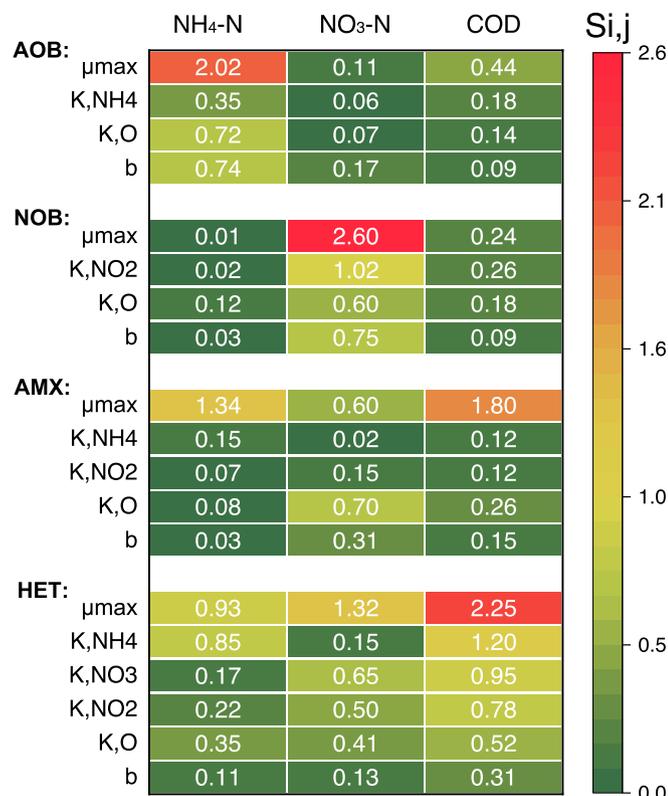
Fig. 2. Sensitivity analysis of the N components and COD by different kinetic parameters.

(0.2–0.4 mg O_2/L) and on/off ratio (0.02–0.3) in the intermittent aeration. The sum of the aeration and non-aeration periods was fixed on 20 min in the 12-hour reaction cycle of SBR, e.g., the on/off ratio of 0.05 refers to 1 min on and 19 min off periods (optimized values). Optimization was carried out using the GSP-X optimizer utility in the long-term during the calibrated period. The results were evaluated in terms of maximizing daily averages of NRR and NRE (calculated based on TIN) as the optimization target variable. All 18 defined scenarios for the analysis were presented (see supplementary material).

2.4.5. Correlation of process parameters using PCA

PCA is a useful analytical tool to understand the link between process parameters and reactor performance and classify data based on their stated variables in a variety of domains. PCA creates a new set of variables, and the old variables are transformed orthogonally. Different environmental effects are represented by arrows, with the length of the arrow indicating the degree of the factor. A positive correlation between two corresponding environmental elements is indicated by an acute angle between two arrows, and a negative correlation by an obtuse angle (Chen et al., 2021).

The fundamental goal of this multivariate method is to highlight those factors that improve the relative description of other objects, create specific groupings based on similarities, and classify variables (Rezaali et al., 2020). To reduce redundancy, the result contains two or three principal components (PC), which are a linear mixture of the original data plus orthogonal eigenvectors (Ringnér, 2008), to compare statistical relationships between operational parameters (MLSS, temperature, pH and DO), influent/effluent NH_4-N, and effluent NO_3-N. The two-dimensional (2D) PCA was created by OriginPro 2021 (OriginLab Corp) with a statistically significant level ($p < 0.05$).

Table 2
List of the kinetic parameters adjusted during calibration.

Bacteria	parameter	Unit	Initial value (Table 1)	Adjusted value
AOB	μ_{AOB}	1/d	1.01	0.5
	$K_{O,AOB}$	mg O_2/L	0.30	0.35
NOB	μ_{NOB}	1/d	0.31	0.3
	$K_{O,NOB}$	mg O_2/L	0.2	0.23
HET	μ_{HET}	1/d	2.0	1.0
AMX	μ_{AMX}	1/d	0.03	0.025

AOB: Ammonia oxidation bacteria, NOB: Nitrite oxidation bacteria, HET: Heterotroph bacteria, AMX: Anammox, K: half-saturation coefficient, μ: Maximum specific growth rate, and b: Decay rate.
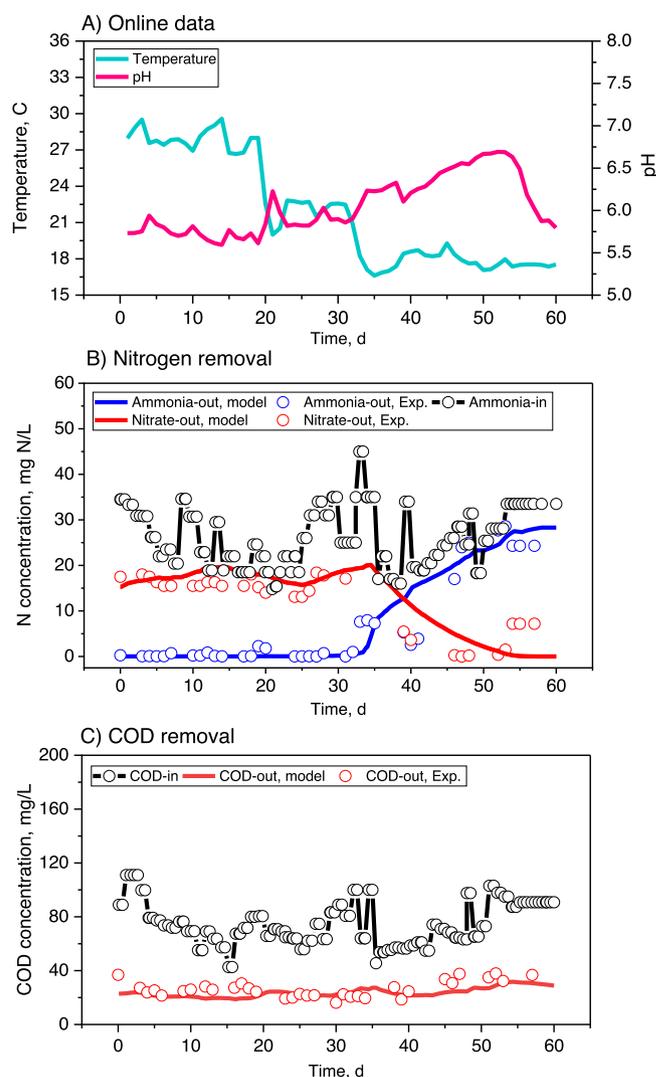

Fig. 3. Calibration results during the winter season (with temperature adaptation in the first 20 days of calibration period): A) online variables, B) concentrations of N components, and C) COD concentrations.

3. Results and discussion

3.1. Sensitivity analysis

Fig. 2 shows the sensitivity coefficients for all 19 kinetic parameters related to AOB, NOB, anammox (AMX), and heterotroph bacteria (HET)
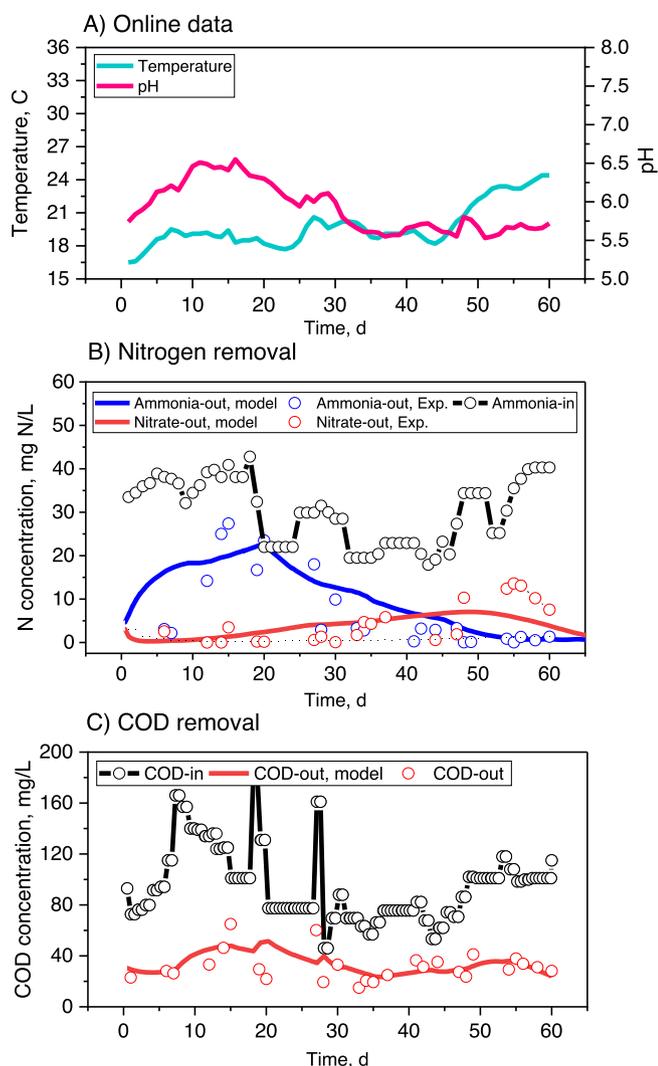
A) Online data

B) Nitrogen removal

C) COD removal

Fig. 4. Validation results during the summer season (without temperature adaptation), A) online variables, B) concentrations of N components, and C) COD concentrations.

concerning three state variables in the effluent tank (NH$_4$-N, NO$_3$-N, and COD). The μ of AOB, NOB, and HET were extremely influential ($S_{i,j} \geq 2$) for NH$_4$-N, NO$_3$-N, and COD, respectively. Next, high influential parameters ($1.0 \leq S_{i,j} < 2.0$) comprised K$_{NO2-N}$ of NOB for NO$_3$-N, μ_{AMX} for NH$_4$-N and COD, μ_{HET} for NO$_3$-N, and K$_{NH4-N}$ of HET for COD. The μ_{AMX} was the most influential kinetic parameter concerning the behavior of NH$_4$-N, with the $S_{i,j}$ ranging from 1.3 to 1.8. On the other hand, the decay rates of AMX and HET were among the least influential parameters.

3.2. Model calibration (parameter estimation)

Overall, μ of all the bacterial groups and Ko of AOB and NOB were

Table 3
A summary of the model efficiency measures during the calibration and validation phases.

State variables	Calibration phase			Validation phase		
	R^2	RMSE	MAE	R^2	RMSE	MAE
NH$_4$-N	0.85	2.29	2.75	0.79	3.67	4.02
NO$_3$-N	0.78	3.47	3.61	0.74	4.10	4.81
COD	0.88	2.36	2.95	0.76	3.72	3.45

among the highly influential parameters (Si,j > 1.0) and were thus selected for estimation in the calibration procedure, while the remaining parameters were kept constant based on the results of previous studies (Yu et al., 2020; Al-Hazmi et al., 2021). Table 2 presents the adjusted values of the kinetic parameters.

The experimental data and calibrated model predictions for the most important variables in the system (NH$_4$-N, NO$_3$-N, and COD) are shown in Fig. 3. The temperature was 27–30 °C during the first 20 days, which was the adaptation period. Subsequently, the temperature was not controlled, and the reactor was kept at ambient temperature, decreasing to 16 °C (Fig. 3a). The pH value was kept in the range of 5.7–6.7 (with an average of 6.2 and a standard deviation of 2.5 mg/L) throughout the operation (Fig. 3a). Other studies also demonstrated the possibility of nitrification in low pH conditions in biofilm reactors (Tarre et al., 2007). Another study also proved that the acidic operation of a nitrifying bioreactor in the pH range of 5 – 6 can generate ppm level free nitrous acid (FNA), as an inhibitor for the suppression of NOB activity (Li et al., 2020). Besides, the inhibitory effect of FNA on anammox bacteria is not comprehensively understood. But it is shown that active anammox bacteria may sustain in various acidic aquatic environments with pH 3.9 – 6.5 (Nie et al., 2018).

The influent NH$_4$-N concentration during calibration was in the range of 18–45 mg/L with the average and standard deviation of 30 mg/L and 2.3 mg/L, respectively. The calibrated model simulated the effluent concentration of NH$_4$-N and NO$_3$-N very well (Fig. 3b). There was a stable operation of the system in the first 30 days for NH$_4$-N removal with an NH$_4$-N effluent concentration of < 1 mg/L. In the same period, NO$_3$-N production occurred with a concentration of up to 20 mg/L. The nitrifier population is subjected to substantial changes because of the reduction of μ_{AOB} and μ_{NOB} which is the function of the temperature. Due to the operational and natural conditions, the temperature decreased to ambient condition (Fig. 3b). In the same period, the negligible concentration of NH$_4$-N in the effluent started to increase, and consequently, NO$_3$-N decreased to zero. As shown in Fig. 3c, COD in the influent was always below 120 mg/L with the average and standard deviation of 80 mg/L and 2.0 mg/L. COD removal was stable (60–70%) during the entire calibration period and was not subjected to any change after dropping the temperature.

Comparing the adjusted model parameters (Table 2) implies that μ_{AOB} was reduced by approximately 50% and there was only a slight change in μ_{NOB} compared to the initial values (Table 1). The adjusted values for μ_{AOB} (0.5 1/d) and μ_{NOB} (0.3 1/d) are in accordance with the results of other studies (Park et al., 2017; Zhang et al., 2019). Neither K$_{O,AOB}$, nor K$_{O,NOB}$ was subjected to any significant change after calibration and remained in the reported range (Mehrani et. al. 2021). Moreover, μ_{HET} was reduced from its initial value of 2.0 1/d to 1.0 1/d and μ_{AMX} was modified from 0.03 to 0.025 1/d.

3.3. Model validation

For model validation, a different set of experimental data was examined (April-June). Fig. 4 shows the observed data and model predictions of NH$_4$-N, NO$_3$-N, and COD during the validation phase. The temperature during the validation period was more stable (varied averagely between 16 and 19.5 °C) up to the last 10 days of the simulation period. From day 45 of validation, the temperature increased naturally up to 24 °C during the summer conditions (June) in Germany.

During the validation period, the minimum and maximum influent NH$_4$-N concentrations were 18 and 44 mg/L with the average and standard deviation of 30 mg/L and 2.5 mg/L. The NH$_4$-N concentration in the effluent gradually reduced after day 20 of the validation and from day 40 to 60 of validation, the NH$_4$-N in the effluent was stable (<5 mg/L). The validated model could predict this gradual decrease and stability (Fig. 4b). The NO$_3$-N concentration was kept below 10 mg N/L and the model predicted it accurately. By increasing the temperature in summer, NO$_3$-N increased by 5 mg N/L and NH$_4$-N decreased to nearly zero
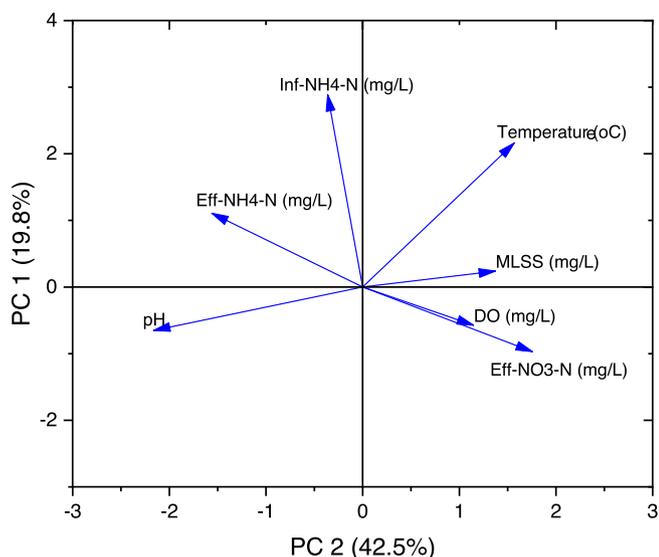
Fig. 5. Relationship between operational parameters and N components by PCA.

(Fig. 4b). Concerning the COD, the influent concentration in the first 30 days of the validation period was fluctuated up to 160 mg/L for a few days (average and standard deviation as 90 mg/L and 3.1 mg/L). The validated model could fit the measurements of the COD in the effluent as well (Fig. 4c).

3.4. Model efficiency evaluation

Numerical values for all the model efficiency measures (R^2, RMSE, MAE) are listed in Table 3. The model appears to have a high goodness-of-fit ($R^2 > 0.8$) in the calibration phase for all the evaluated variables (NH_4-N, NO_3-N, and COD). Moreover, a reasonable goodness-of-fit ($R^2 > 0.7$) was achieved for all the variables in the validation phase, revealing the accurate performance of the model.

3.5. Correlation of process parameters by PCA

PCA was employed as a useful analytical method to explore the link between process parameters. PC1 axis with 42.5% variance is more significant criterion rather than the PC2 axis (19.8%) for comparing various parameters correlation. The arrows reflect several environmental factors, while the length of the arrow is representing the degree of the element (Fig. 5). The effluent NO_3-N was closely correlated with the DO value, showing the importance of the aeration strategy for efficient NOB suppression. MLSS showed a positive correlation with NO_3-N, while a direct negative correlation between NO_3-N and NH_4-N in the effluent can be seen. Both pH and temperature were less correlated with the effluent NO_3-N.

3.6. Optimization of the aeration strategy

Fig. 6 shows the optimization of the aeration strategy including the DO values (0.2 to 0.4 mg/L) and on/off ratio (0.05–0.3) considering on daily average of NRR and NRE, NH_4-N, and COD removal efficiency. Overall, the optimum values for DO and on/off ratio were obtained 0.2–0.25 mg O_2/L and 0.05 (Aeration pump is 1.0 min on per each the

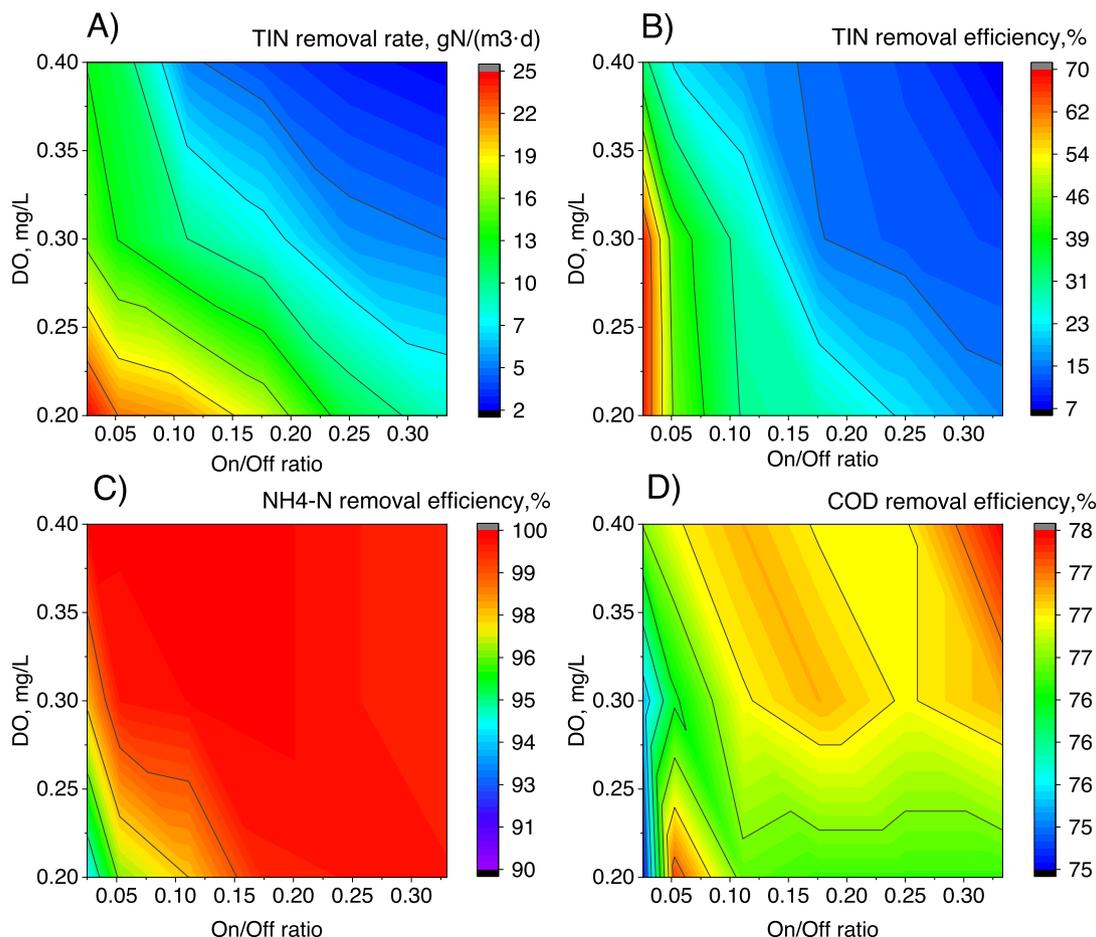**Fig. 6.** Optimization of the aeration strategy, A) NRR for TIN, B) NRE for TIN, C) NRE for NH_4-N, and D) COD removal efficiency (all results as the daily average).

Table 4
Summary of different aeration strategy optimization techniques and results in different N removal systems and the comparison with this study.

Optimization method	Optimization factors	Optimization target	Process (System)	Remarks
Experimental (Lochmatter et al., 2013)	DO set-point and aeration type (intermittent or alternating high/low DO)	Maximizing the N and P removal efficiency	N-DN (SBR)	The maximum NRE was achieved using intermittent aeration rather than alternatively high/low DO. Intermittent aeration with anoxic periods and without mixing between aeration pulses was significantly better for N-removal (78.3%) with the lowest COD loading rate examined.
Data-driven (Asadi et al., 2017)	DO set point	Reducing energy consumption without affecting the effluent quality	N-DN (WWTP)	The optimization caused increasing the effluent quality such as BOD, and TSS up to 18% (even better than actual values).
RSM (Leix et al., 2017)	DO set-point (including change in anoxic and aeration modes) and stripping effects.	Maximizing the NRR and minimizing N_2O emissions	PN/A (SBR)	The most appropriate condition was intermittent aeration with equally distributed aerated (5.5 min) and unaerated phases (6.5 min) at a moderate aeration intensity (44 L/h).
CFD (Zhou et al., 2019)	DO set-point and aeration intensity	Maximizing the TN removal and reactor stability	PN/A (bioreactor)	An optimized low DO of 0.2 mg O_2/L and high aeration intensity (0.17 cm/s) resulted in denitrifying bacteria growth and high TN removal (82.1%) and a persistent biofilm structure.
Experimental (Yang et al., 2020)	DO set-point	Efficient N removal, and stable AOB and anammox activity	PN/A (IFAS)	The optimized DO was in a range of 0.24–0.28 mg O_2/L, caused the stable AOB activity and enhanced ammonia and TN removal. When the DO was in the range of 0.28–0.35 mg O_2/L, the anammox activity was inhibited and a considerable amount of free nitrous acid (FNA) was accumulated (21.70 µg/L).
Experimental (Xu et al, 2020)	DO set-point and anoxic/aerobic ratio	Maximizing the NRR, NRE, and NOB suppression	PN/A (IFAS)	For NOB suppression, the DO value was more significant than the anoxic period. By optimizing the intermittent aeration (low DO of 0.5 mg O_2/L and anoxic time of 20 min), the NRR was enhanced by 40%, a steady and high NRE (80–89%) was achieved, and NOB was more inhibited with a low DO level (0.5 mg O_2/L), rather than a high DO of 1.5–1.8 mg O_2/L.
Mechanistic model (Al-Hazmi et al., 2021)	DO set-point, on/off frequently, and on/off ratio	Maximizing the AUR, minimizing the NPR and N2O emission	PN/A (SBR)	High AUR to low NPR values (NPR/AUR = 0.07–0.08) and limited N_2O emissions (E_{N2O} < 2%) were achieved at the optimized aeration parameters (DO set-point = 0.7 mg O_2/L, on/off ratio of 2, and on/off frequency of 6–7 h^{-1}).
Mechanistic model (long-term optimization (this study)	DO set-point and on/off ratio	Maximizing the NRR and NRE for TIN and NOB suppression	PN/A (IFAS-SBR)	Aeration optimization was done in a long-term 30 days of the operation. The optimized values of DO (0.2–0.25 mg O_2/L), and on/off ratio of 0.05 (1 min on and 19 min off) could enhance the daily average values from 30% to > 50% (NRE), and from 15 g N/m^3.d to ~ 25 g N/m^3.d (NRR).

PN/A: partial nitrification/anammox (deammonification), N-DN: nitrification–denitrification, NRR: N removal rate, NRE: N removal efficiency, TIN: total inorganic nitrogen, RSM: response surface methodology, CFD: computational fluid dynamics, AUR: ammonium utilization rate, NPR: nitrate production rate.

20 min cycle), respectively to achieve the highest NRR and NRE of the system. By decreasing of DO and on/off ratio (up to 0.2–0.25 mg/L and 0.05), the current levels of NRE and NRR could increase from the daily average of 30% to > 50% and from 15 g N/m^3.d to approximately 25 g N/m^{3}d, respectively (Fig. 6a,b). However, the optimization did not have a significant individual effect on NH$_4$-N and COD removal efficiently (Fig. 6c,d).

Moreover, Table 4 provided a summary of recent optimization studies in N removal systems and a comparison of them with this study. As stated, most of the past studies on aeration strategy optimization were carried out in short-term operational conditions while this study investigated optimization under the long-term period of 30 days. The DO set-point and aeration on/off times were two important optimization factors, while maximizing the NRR and NRE, stable suppression of NOB, and mitigation of N$_2$O production were among the most important optimization target in such studies.

Lochmatter et al., (2013) optimized an aeration strategy and reported that highest NRE can be achieved by intermittent aeration rather than DO setpoint. Nevertheless, Asadi et al., 2017 and Zhou et al., (2019) built optimize-based models on DO setpoint and aeration intensity. Furthermore, Leix et al., (2017) optimized intermittent aeration mode (stripping effect and aerated/unaerated phases) to maximize the NRR and minimize N$_2$O emissions using the response surface methodology (RSM).

Yang et al., (2020) noted that the optimized DO (0.24–0.28 mg O$_2$/L) could enhance ammonia and TN removal with the stable AOB activity in a deammonification process in an IFAS system. Xu et al., (2020) revealed that optimization of the intermittent aeration (low DO of 0.5 mg O$_2$/L and anoxic time of 20 min), can improve the NRR by 40% and achieved a high NRE (80–89%). Very recently, Al-Hazmi et al., (2021), optimized aeration (DO set-point, on/off frequently, and ratio) of the deammonification process in a laboratory-scale SBR. High ammonia utilization rate (AUR), low nitrite production rate (NPR), and limited N$_2$O emissions (N$_2$O emission factor < 2%) were achieved at the optimized aeration parameters (DO set-point = 0.7 mg O$_2$/L, aeration on/off ratio of 2, and on/off frequency of 6–7 h^{-1}). The optimized aeration value of this study (DO set-point of 0.2–0.25 mgO$_2$/L, and on/off ratio of 0.05) are in range within the reported range of Zhou et al., (2019), and Yang et al., (2020). This low DO value and on/off ratio not only can enhance the NRE and NRR value (up to 50%), but also can improve the reactor performance, and energy saving of the system (Hreiz et al., 2015; Wang et al., 2022).

In the end, some recent intermittent aeration strategies in successful deammonification systems were compared (see supplementary material). The DO ranges are between 0.2 and 0.5 mg O$_2$/L and aeration time varies between 2 and 40 min. In an intermittent aeration system, NOB inhibition was related to the DO concentration, anoxic time, and parameters, such as the type of NOB species (Bao et al., 2017). A recent study showed that a 15-minute anoxic interval suppressed NOB activity, which could be due to the high concentrations of free ammonia in the influent (Qiu et al., 2019). Besides, high nitrite accumulation could be sustained at a high DO (>1.5 mg O$_2$/L) under intermittent aeration (Regmi et al., 2014).

To summarize, the outcomes of this modelling and optimization study provided insights into the operational condition of mainstream deammonification systems under dynamic temperature and COD: N ratio and the effect of intermittent aeration optimization on N-removal efficiency and NOB suppression performance.

4. Conclusions

A mechanistic model for the mainstream deammonification process in temperature variations was successfully verified using real pilot-scale data. The aeration strategy optimization showed by decreasing the DO set-point and on/off ratio to 0.2 mg O$_2$/L and 0.05, respectively, the NRR and NRE increased up to 25 g N/m^3.d and > 50%. PCA results confirmed that the DO set-point and on/off ratio are the most crucial parameters in

the suppression of NOB. Overall, the novel long-term optimization strategy of this research is a powerful tool for enhancing the efficiency and the effluent quality of the mainstream deammonification.

CRediT authorship contribution statement

Mohamad-Javad Mehrani: Conceptualization, Investigation, Methodology, Formal analysis, Visualization, Data curation, Software, Validation, Writing – original draft. **Mohammad Azari:** Conceptualization, Investigation, Methodology, Data curation, Visualization, Writing – review & editing. **Burkhard Teichgräber:** Resources, Project administration, Writing – review & editing. **Peter Jagemann:** Resources, Project administration, Funding acquisition, Writing – review & editing. **Jens Schoth:** Conceptualization, Methodology, Writing – review & editing. **Martin Denecke:** Resources, Project administration, Funding acquisition, Writing – review & editing. **Jacek Mąkinia:** Resources, Methodology, Supervision, Funding acquisition, Writing – review & editing.

Declaration of Competing Interest

The authors declare that they have no known competing financial interests or personal relationships that could have appeared to influence the work reported in this paper.

Appendix A. Supplementary data

Supplementary data to this article can be found online at https://doi.org/10.1016/j.biortech.2022.126942.

References

Abou-Elela, S.I., Hamdy, O., El Monayeri, O., 2016. Modeling and simulation of hybridanaerobic/aerobic wastewater treatment system. Int. J. Environ. Sci. Tech. 13 (5), 1289–1298.

Al-Hazmi, H.E., Lu, X., Majtacz, J., Kowal, P., Xie, L., Makinia, J., 2021. Optimization of the aeration strategies in a deammonification sequencing batch reactor for efficient nitrogen removal and mitigation of N2O production. Environ. Sci. Tech. 55 (2), 1218–1230.

Asadi, A., Verma, A., Yang, K., Mejabi, B., 2017. Wastewater treatment aeration process optimization: A data mining approach. J. Environ. Manage. 203, 630–639.

Azari, M., Aslani, A., Denecke, M., 2020. The effect of the COD: N ratio on mainstream deammonification in an integrated fixed-film activated sludge sequencing batch reactor. Chemosphere 259, 127426. https://doi.org/10.1016/j.chemosphere.2020.127426.

Azari, M., Jurnalis, A., Denecke, M., 2021. The influence of aeration control and temperature reduction on nitrogen removal and microbial community in two anammox-based hybrid sequencing batch biofilm reactors. J. Chem. Tech. Biotech. 96 (12), 3358–3370.

Baeten, J.E., Batstone, D.J., Schraa, O.J., van Loosdrecht, M.C.M., Volcke, E.I.P., 2019. Modelling anaerobic, aerobic and partial nitritation-anammox granular sludge reactors - A review. Water Res. 149, 322–341.

Batstone, D.J., Keller, J., Angelidaki, I., Kalyuzhnyi, S.V., Pavlostathis, S.G., Rozzi, A., Sanders, W.T.M., Siegrist, H.A., Vavilin, V.A., 2002. The IWA anaerobic digestion model no 1 (ADM1). Water Science and technology 45 (10), 65–73.

Chang, K.-H., 2012. Stochastic Nelder-Mead simplex method – A new globally convergent direct search method for simulation optimization. Euro.J. Opera. Res. 220 (3), 684–694.

Chen, J., Zhou, X., Cao, X., Li, S., 2021. Optimizing anammox capacity for weak wastewater in an AnSBBR using aerobic activated sludge as inoculation. J. Environ. Manage. 280, 111649.

Gao, D., Xiang, T., 2021. Deammonification process in municipal wastewater treatment: Challenges and perspectives. Bioresour. Tech. 320, 124420.

Gu, J., Zhang, M., Liu, Y., 2020. A review on mainstream deammonification of municipal wastewater: Novel dual step process. Bioresour. Tech. 299, 122674.

Guven, H., Ersahin, M.E., Dereli, R.K., Ozgun, H., Isik, I., Ozturk, I., 2019. Energy recovery potential of anaerobic digestion of excess sludge from high-rate activated sludge systems co-treating municipal wastewater and food waste. Energy 172, 1027–1036.

Han, M., Vlaeminck, S.E., Al-Omari, A., Wett, B., Bott, C., Murthy, S., De Clippeleir, H., 2016. Uncoupling the solids retention times of flocs and granules in mainstream deammonification: A screen as effective out-selection tool for nitrite oxidizing bacteria. Bioresour. Tech. 221, 195–204.

Hausherr, D., Niederdorfer, R., Morgenroth, E., Joss, A., 2021. Robustness of mainstream anammox activity at bench and pilot scale. Sci. Total Environ. 796, 148920. https://doi.org/10.1016/j.scitotenv.2021.148920.

Henze, M., Gujer, W., Mino, T., Matsuo, T., Wentzel, M.C., Marais, G.V.R., Van Loosdrecht, M.C., 1999. Activated sludge model no. 2d, ASM2d. Water science and technology 39 (1), 165–182.

Hong, Y., Liao, Q., Bonhomme, C., Chebbo, G., 2019. Physically-based urban stormwater quality modelling: An efficient approach for calibration and sensitivity analysis. J. Environ. Manage. 246, 462–471.

Hreiz, R., Latifi, M.A., Roche, N., 2015. Optimal design and operation of activated sludge processes: State-of-the-art. Chem. Eng. J. 281, 900–920.

Izadi, P., Izadi, P., Eldyasti, A., 2021. Towards mainstream deammonification: Comprehensive review on potential mainstream applications and developed sidestream technologies. J. Environ. Manage. 279, 111615.

Jimenez, J., Miller, M., Bott, C., Murthy, S., De Clippeleir, H., Wett, B., 2015. High-rate activated sludge system for carbon management – Evaluation of crucial process mechanisms and design parameters. Water Res. 87, 476–482.

Leix, C., Drewes, J.E., Ye, L., Koch, K., 2017. Strategies for enhanced deammonification performance and reduced nitrous oxide emissions. Bioresour. Tech. 236, 174–185.

Lemaire, R., Christensson, M., 2021. Lessons Learned from 10 Years of ANITA Mox for Sidestream Treatment. Processes 9 (5), 863.

Li, J., Xu K., Liu, T., Bai, G., Liu, Y. 2020. Chengwen Wang, Min Zheng. 2020. Achieving Stable Partial Nitration in an Acidic Nitrifying Bioreactor. *Environmental Science & Technology* 54 (1), 456-463.

Lochmatter, S., Gonzalez-Gil, G., Holliger, C., 2013. Optimized aeration strategies for nitrogen and phosphorus removal with aerobic granular sludge. Water Res. 47 (16), 6187–6197.

Malovanyy, A., Trela, J., Plaza, E., 2015. Mainstream wastewater treatment in integrated fixed film activated sludge (IFAS) reactor by partial nitritation/anammox process. Bioresour. Tech. 198, 478–487.

Mehrani, M.-J., Lu, X., Kowal, P., Sobotka, D., Mąkinia, J., 2021. Incorporation of the complete ammonia oxidation (comammox) process for modeling nitrification in suspended growth wastewater treatment systems. J. Environ. Manage. 297, 113223.

Mehrani, M.-J., Sobotka, D., Kowal, P., Ciesielski, S., Makinia, J., 2020. The occurrence and role of Nitrospira in nitrogen removal systems. Bioresour. Tech. 303, 122936.

Miao, Y., Zhang, L., Yang, Y., Peng, Y., Li, B., Wang, S., Zhang, Q., 2016. Start-up of single-stage partial nitrification-anammox process treating low-strength swage and its restoration from nitrate accumulation. Bioresour. Tech. 218, 771–779.

Newhart, K.B., Holloway, R.W., Hering, A.S., Cath, T.Y., 2019. Data-driven performance analyses of wastewater treatment plants: A review. Water Res. 157, 498–513.

Nie, S., Lei, X., Zhao, L., Wang, Y.i., Wang, F., Li, H.u., Yang, W., Xing, S., 2018. Response of activity, abundance, and composition of anammox bacterial community to different fertilization in a paddy soil. Biology and Fertility of Soils 54 (8), 977–984.

Park, M.-R., Park, H., Chandran, K., 2017. Molecular and kinetic characterization of planktonic nitrospira spp. selectively enriched from activated sludge. Environ. Sci. Tech. 51 (5), 2720–2728.

Pekyavas, G., Dereli, R.K., Yangin-Gomec, C., 2020. Comparative assessment of modeling and experimental data of ammonia removal from pre-digested chicken manure. J. Environ. Sci. Health, Part A 55 (11), 1333–1338.

Puchongkawarin, C., Gomez-Mont, C., Stuckey, D.C., Chachuat, B., 2015. Optimization-based methodology for the development of wastewater facilities for energy and nutrient recovery. Chemosphere 140, 150–158.

Qiao, J., Zhang, W., 2018. Dynamic multi-objective optimization control for wastewater treatment process. Neural Computing and Applications 29 (11), 1261–1271.

Qiu, S., Hu, Y., Liu, R., Sheng, X., Chen, L., Wu, G., Hu, H., Zhan, X., 2019. Start up of partial nitritation-anammox process using intermittently aerated sequencing batch reactor: Performance and microbial community dynamics. Sci. Total Environ. 647, 1188–1198.

Regmi, P., Miller, M.W., Holgate, B., Bunce, R., Park, H., Chandran, K., Wett, B., Murthy, S., Bott, C.B., 2014. Control of aeration, aerobic SRT and COD input for mainstream nitritation/denitritation. Water Res. 57, 162–171.

Rezaali, M., Karimi, A., Moghadam Yekta, N., Fouladi Fard, R., 2020. Identification of temporal and spatial patterns of river water quality parameters using NLPCA and multivariate statistical techniques. Int. J. Environ. Sci. Tech. 17 (5), 2977–2994.

Ringnér, M., 2008. What is principal component analysis? Nature Biotech. 26 (3), 303–304.

Sean, W.-Y., Chu, Y.-Y., Mallu, L.L., Chen, J.-G., Liu, H.-Y., 2020. Energy consumption analysis in wastewater treatment plants using simulation and SCADA system: Case study in northern Taiwan. J. Clean. Prod. 276, 124248.

Tarre, S., Shlafman, E., Beliavski, M., Green, M., 2007. Changes in ammonia oxidiser population during transition to low pH in a biofilm reactor starting with Nitrosomonas europaea. Water Sci. Tech. 55 (8–9), 363–368.

Van Hulle, S.W.H., Vandeweyer, H.J.P., Meesschaert, B.D., Vanrolleghem, P.A., Dejans, P., Dumoulin, A., 2010. Engineering aspects and practical application of autotrophic nitrogen removal from nitrogen rich streams. Chem. Eng. J. 162 (1), 1–20.

Waqas, S., Bilad, M.R., Man, Z., Wibisono, Y., Jaafar, J., Indra Mahlia, T.M., Khan, A.L., Aslam, M., 2020. Recent progress in integrated fixed-film activated sludge process for wastewater treatment: A review. J. Environ. Manage. 268, 110718.

Wang, L., Gu, W., Liu, Y., Liang, P., Zhang, X., Huang, X., 2022. Challenges, solutions and prospects of mainstream anammox-based process for municipal wastewater treatment. Sci. Total Environ. 820, 153351.

Xu, Z., Zhang, L., Gao, X., Peng, Y., 2020. Optimization of the intermittent aeration to improve the stability and flexibility of a mainstream hybrid partial nitrification-anammox system. Bioresour. Tech. 261, 127670.

Yang, S., Xu, S., Boiocchi, R., Mohammed, A., Li, X., Ashbolt, N.J., Liu, Y., 2020. Long-term continuous partial nitration-anammox reactor aeration optimization at different nitrogen loading rates for the treatment of ammonium rich digestate lagoon supernatant. Process Biochem. 99, 139–146.

Yu, L., Chen, S., Chen, W., Wu, J., 2020. Experimental investigation and mathematical modeling of the competition among the fast-growing "r-strategists" and the slow-growing "K-strategists" ammonium-oxidizing bacteria and nitrite-oxidizing bacteria in nitrification. Sci. Total Environ. 702, 135049. https://doi.org/10.1016/j.scitotenv.2019.135049.

Zhang, Q., Li, Z., Snowling, S., Siam, A., El-Dakhakhni, W., 2019. Predictive models for wastewater flow forecasting based on time series analysis and artificial neural network. Water Sci. Tech. 80 (2), 243–253.

Zhou, J.h., Yu, H.c., Ye, K.q., Wang, H.y., Ruan, Y.j., Yu, J.m. 2019. Optimized aeration strategies for nitrogen removal efficiency: application of end gas recirculation aeration in the fixed bed biofilm reactor. Environmental Science and Pollution Research, 26(27), 28216-28227.